Investigation of Copper(I) Oxide Quantum Dots by Near-Edge X-ray Absorption Fine Structure Spectroscopy

Ponnusamy Nachimuthu,[†,‡] Suntharampillai Thevuthasan,*[,§] Yong J. Kim,[||] Alan S. Lea,[§] Vaithiyalingam Shutthanandan,[§] Mark H. Engelhard,[§] Donald R. Baer,[§] Scott A. Chambers,[§] David K. Shuh,[‡] Dennis W. Lindle,[†] Eric M. Gullikson,[‡] and Rupert C. C. Perera[‡]

Department of Chemistry, University of Nevada, Las Vegas, Nevada 89154, Lawrence Berkeley National Laboratory, Berkeley, California 94720, Pacific Northwest National Laboratory, Richland, Washington 99352, and Department of Chemical Technology, Hanbat National University, Taejon, Korea

Received January 7, 2003. Revised Manuscript Received May 21, 2003

Copper(I) oxide quantum dots (OQDs) were grown in various thicknesses on different $SrTiO_3$(001) surfaces and were investigated by near-edge X-ray absorption fine structure (NEXAFS) spectroscopy. The experimental growth conditions for the OQDs were optimized to obtain Cu_2O as the major phase. The OQDs grown on clean $SrTiO_3$(001) surfaces at 825 K and higher with $p(O_2)$ of 9.0×10^{-7} Torr or greater contain mostly CuO, contrasting to OQDs grown at 800 K with $p(O_2)$ of $\sim 7.0 \times 10^{-7}$ Torr that contain primarily Cu_2O. Furthermore, there is a strong interaction between the $SrTiO_3$(001) surface and the first few monolayers of the OQDs, which induces the formation of Cu(II). However, this interaction is mitigated with increasing thickness of OQDs, resulting in the exclusive formation of Cu_2O in the topmost layers. The influence of the $SrTiO_3$(001) substrate on the formation of OQDs can be minimized by modifying the substrate surface using chemical treatment and/or energetic Au^{2+} ion-beam irradiation. Examination of the photochemical properties of these OQDs shows that prolonged soft X-ray irradiation under vacuum reduces Cu(II), which is present as a minor impurity in the Cu(I) OQDs.

Introduction

Interface-controlled nucleation and growth of two- and three-dimensional nanostructures results in structures possessing unique structural, optical, electronic, and vibrational properties derived from the quantum confinement of charge carriers. When sufficiently small, three-dimensional quantum-dot structures display atom-like discrete energy levels, and recent investigations have focused on tailoring these size effects for semiconductor technology, especially for electronic and optoelectronic applications.[1−9] Spontaneous self-assembled island formation results from the lattice mismatch between the two materials used in this investigation and provides the basis for the nucleation of these quantum dots. However, many aspects of the formation of these structures are unknown. In many cases, molecular beam epitaxy (MBE) and chemical vapor deposition (CVD) methods have been used to generate semiconductor quantum dots on suitable substrates.[3−6,8,9] Although there has been success in the formation of semiconductor quantum dots, characterization of these materials and structures using conventional surface science techniques has been a challenge. Most semiconductor quantum dots are sensitive to the environment in which they are stored and, as such, special attention is needed either to passivate the surfaces or to keep the structures in an inert environment. Procedures used to protect the semiconductor quantum dots limit their technological utility. Thus, development of these structures using more robust materials is necessary. Oxide materials are frequently more chemically stable under various environments compared to conventional semiconductor materials that might be used for quantum dots. Oxides also constitute a highly diverse class of materials with rich optical, electronic, magnetic, and dielectric properties. Thus, chemically stable oxide nanostructures may ex-

* Corresponding author. Phone: 509 376 1375. Fax: 509 376 5106. E-mail: theva@pnl.gov.
[†] University of Nevada, Las Vegas.
[‡] Lawrence Berkeley National Laboratory.
[§] Pacific Northwest National Laboratory.
[||] Hanbat National University, Korea.

(1) Zinke-Allmang, M.; Feldman, L. C.; Grabow, M. H. *Surf. Sci. Rep.* **1992**, *16*, 377.
(2) Notzel, R. *Semicond. Sci. Technol.* **1996**, *11*, 1365.
(3) Xin, S. H.; Wang, P. D.; Yin, A.; Kim, C.; Dobrowolska, M.; Merz, J. L.; Furdyna, J. K. *Appl. Phys. Lett.* **1996**, *69*, 3884.
(4) Flack, F.; Samarth, N.; Nikitin, V.; Crowell, P. A.; Shi, J.; Levy, J.; Awschalom, D. D. *Phys. Rev. B* **1996**, *54*, 17312.
(5) Guryanov, G. M.; Cirlin, G. E.; Pterov, V. N.; Polyakov, N. K.; Golubok, A. O.; Tipissev, S. Y.; Gubanov, V. B.; Samsonenko, Y. B.; Ledentsov, N. N.; Shchukin, V. A.; Grundmann, M.; Bimberg, D.; Alferov, Z. I. *Surf. Sci.* **1996**, *352*, 651.
(6) Ko, H. C.; Park, D. C.; Kawakami, Y.; Fujita, S.; Fujita, S. *Appl. Phys. Lett.* **1997**, *70*, 3278.
(7) Daruka, I.; Barabasi, A. L. *Appl. Phys. Lett.* **1998**, *72*, 2102.
(8) Lee, S.; Daruka, I.; Kim, C. S.; Barabsi, A. L.; Merz, J. L.; Furdyna, J. K. *Phys. Rev. Lett.* **1998**, *81*, 3479.
(9) Medeiros-Riberiro, G.; Bratkovski, A. M.; Kamins, T. I.; Ohlberg, D. A. A.; Williams, R. S. *Science* **1998**, *279*, 353.

10.1021/cm021757n CCC: $25.00
Published on Web 09/05/2003

hibit multiple functionalities and, as such, have significant technological potential. Despite this promise, oxide quantum dots (OQDs) have received much less attention, and the growth and characterization of OQDs is relatively unexplored.

Copper oxides are known to exist in two semiconducting phases, the first of which is cupric oxide (Cu(II), CuO) and the other is cuprous oxide (Cu(I), Cu_2O). In addition to their unique electronic structures,[10] copper oxide nanostructures, especially Cu(I) OQDs, can be used effectively in chemical and photochemical applications; for example, the photocatalytic decomposition of water into H_2 and O_2 on Cu_2O under visible light irradiation has recently been demonstrated.[11] Recent investigations of the growth and characterization of these nanostructures on several substrates found formation of OQDs in various sizes containing CuO, Cu_2O, or a mixture of phases.[12−17] During photoexcitation of some specific nanoscale oxide heterojunctions, charge separation is possible between the nanostructures and substrates, and as a result, photochemical activity is greatly enhanced in these systems.[12−17] Cuprous oxide nanostructures on $SrTiO_3$ substrates could exhibit charge separation and enhanced photochemical properties. Thus, a detailed scientific understanding of the growth and characterization of Cu(I) OQDs on $SrTiO_3$(001) surfaces becomes necessary to determine viability of these materials for various photochemical applications. In a previous study, we successfully prepared Cu(I) OQDs on $SrTiO_3$(001) surfaces (with mixed Ti and Sr terminations) and characterized them using atomic force microscopy (AFM), X-ray diffraction, X-ray photoelectron spectroscopy (XPS), and scanning Auger microscopy.[18]

The availability of synchrotron-radiation sources for X-ray absorption spectroscopic measurements has made near-edge X-ray absorption fine structure (NEXAFS) a powerful tool for a detailed understanding of electronic and structural properties of materials.[19−21] NEXAFS is an atom-specific technique capable of probing short- to medium-range structure around an imbedded or absorbing atom. Features in NEXAFS spectra are very sensitive to the local electronic structure and the symmetry of adsorbates, which in turn provide information on the degree of interaction between the surface and adsorbates. Among the experimental techniques employed in determining the oxidation state of an atom in a solid, NEXAFS plays a crucial role due to its simplicity and near-universal applicability. Therefore, NEXAFS has been utilized to characterize copper oxide nanostructures grown on various $SrTiO_3$(001) surfaces. In the present study, using NEXAFS at the Cu $L_{2,3}$- and O K-edges, we have investigated oxidation state and local structure of OQDs grown on several $SrTiO_3$(001) surfaces with different preparation conditions by varying substrate temperature, oxygen partial pressure, and most importantly, the evolution of these properties with varying thicknesses of the nanostructures.

Experimental Section

The OQDs were grown in an oxygen-plasma-assisted-molecular-beam-epitaxial system described elsewhere.[22] Clean surfaces of single-crystal $SrTiO_3$(001) substrates (1 cm × 1 cm × 1 mm) were used as growth templates for the OQDs. In addition, the OQDs were grown on TiO_x-terminated and Au^{2+} ion-implanted surfaces of $SrTiO_3$(001) substrates to investigate the influence of the substrate surface on the formation of OQDs. Prior to the OQDs growth, the TiO_x-terminated surfaces of $SrTiO_3$(001) substrates were obtained by chemical treatments described elsewhere in detail.[23] Regarding the Au^{2+} ion-implanted surface, a single-crystal $SrTiO_3$(001) was irradiated by 2.0 MeV Au^{2+} ions with a fluence of 5.0×10^{14} ions/cm^2 at a temperature of 975 K. Substrates were fastened to the sample holder with Ta clips and a pair of thermocouples was used for temperature measurements. Before growth, the substrates were cleaned using oxygen plasma at a sample temperature of 900 K in 2.0×10^{-5} Torr of oxygen. During the growth, copper was evaporated from an effusion cell at a rate of 6.0×10^{-4} nm/s in the presence of the oxygen plasma. In addition, the oxygen partial pressure in the chamber was maintained at 7.5×10^{-7} Torr while the substrate temperature was varied between 725 and 800 K. Some films were grown at a sample temperature higher than 800 K with oxygen partial pressures in the range of $1.0-1.25 \times 10^{-6}$ Torr to investigate the effect of growth temperature and oxygen partial pressure on OQDs. The growth rate was monitored by quartz crystal oscillators (QCOs) in the MBE system.[22] After growth, several techniques were used to characterize the samples. Rutherford backscattering spectrometry (RBS) along with SIMNRA simulations[24] were used to determine the total copper content in the OQDs. AFM was used to map the topography of the quantum dots while the chemical state information from the surface region of the quantum dots was obtained using synchrotron-radiation-based NEXAFS spectroscopy and laboratory-based XPS.

The NEXAFS spectra of different thicknesses of OQDs grown on $SrTiO_3$(001) surfaces, including TiO_x-terminated and Au^{2+} ion-implanted surfaces with different preparation conditions such as substrate temperature and oxygen partial pressure were collected at Beamline 6.3.2 of the Advanced Light Source (ALS) at the Lawrence Berkeley National Laboratory (LBNL).[25] NEXAFS spectra were also obtained from a series of reference materials to primarily enable the identification of Cu oxidation states in the OQDs. These reference materials included a Cu single crystal cleaned and transferred ex situ into the Beamline 6.3.2 end station (Cu

(10) Zuo, J. M.; Kim, M.; O'Keeffe, M.; Spence, J. C. H. *Nature* **1999**, *401*, 49.
(11) Ikeda, S.; Takata, T.; Kondo, T.; Hitoki, G.; Hara, M.; Kondo, J. N.; Domen, K.; Hosono, H.; Kawazoe, H.; Tanaka, A. *Chem. Commun.* **1998**, 2185. Hara, M.; Kondo, T.; Komoda, M.; Ikeda, S.; Shinohara, K.; Tanaka, A.; Kondo, J. N.; Domen, K. *Chem. Commun.* **1998**, 357.
(12) Orel, B.; Svegi, F.; Bukopvec, N.; Kosec, M. *J. Non-Cryst. Solids* **1993**, *159*, 49.
(13) Kaito, C.; Fujita, K.; Shibahara, H.; Shiojiri, M. *Jpn. J. Appl. Phys.* **1977**, *16*, 697.
(14) Xu, J. F.; Ji, W.; Shen, Z. X.; Tang, S. H.; Ye, X. R.; Jia, D. Z.; Xin, X. Q. *J. Solid State Chem.* **1999**, *147*, 516.
(15) Borgohain, K.; Singh, J. B.; Rama Rao, M. V.; Shripathi, T.; Mahamuni, S. *Phys. Rev. B* **2000**, *61*, 11093.
(16) Das, D.; Chakravorty, D. *Appl. Phys. Lett.* **2000**, *76*, 1273.
(17) Balamurugan, B.; Mehta, B. R.; Shivaprasad, S. M. *Appl. Phys. Lett.* **2001**, *79*, 3176.
(18) Liang, Y.; Lea, A. S.; McCready, D. E.; Meethunkji, P. In *State-of-the-Art Application of Surface and Interface Analysis Methods to Environmental Material Interactions*: *In Honor of James E. Castle's 65th Year*; Baer, D. R., Clayton, C. R., Halada, G. P., Davis, G. D., Eds.; PV, 2001−5; The Electrochemical Society: Washington, D.C., 2001; p 125.
(19) Stöhr, J. *NEXAFS Spectroscopy*; Springer Series in Surface Science, 25; Springer: New York, 1992.
(20) Chen, J. G. *Surf. Sci. Rep.* **1997**, *30*, 5.
(21) de Groot, F. M. F. *Chem. Rev.* **2001**, *101*, 1779.
(22) Chambers, S. A.; Tran, T. T.; Hileman, T. A. *J. Mater. Res.* **1994**, *9*, 2944.
(23) Koster, G.; Kropman, B. L.; Rijnders, G. J. H. M.; Blank, D. H. A.; Rogalla, H. *Appl. Phys. Lett.* **1998**, *73*, 2920.
(24) *SIMNRA User's Guide*; Mayer, M., Ed.; Max-Planck-Institut fur Plasmaphysik: Germany.
(25) Underwood, J. H.; Gullikson, E. M. *J. Electron Spectrosc. Relat. Phenom.* **1998**, *92*, 265.

Table 1. Experimental Conditions Adopted for Growing Copper(I) Oxide Quantum Dots (OQDs) on Different Surfaces of $SrTiO_3$(001) Substrates and the Effective OQD Thickness[a]

$SrTiO_3$(001) surface	substrate temp (K)	oxygen partial pressure, $p(O_2)$ (Torr)	effective OQD thickness (nm)
clean	875	1.2×10^{-6}	2.4
clean	825	9.2×10^{-7}	2.4
clean	800	7.3×10^{-7}	0.6
clean	800	7.1×10^{-7}	1.2
clean	800	7.1×10^{-7}	2.4
clean	800	7.1×10^{-7}	3.6
TiO_x-terminated	800	7.1×10^{-7}	2.4
Au^{2+} ion-implanted	800	7.1×10^{-7}	2.4

[a] The effective OQD thicknesses were determined using the bulk density of Cu_2O coupled with the total Cu content in the OQD measured by QCOs and RBS along with SIMNRA simulations.[24]

metal), a polycrystalline CuO powder [Cu(II)], and a heavily oxidized Cu foil resulting from long-term exposure to the atmosphere [Cu(I)]. During the measurements, the ALS operated at an energy of 1.9 GeV with a storage ring current between 200 and 400 mA. Spectra were recorded near the Cu $L_{2,3}$- and O K-absorption edges in the total electron yield (TEY) detection mode via drain current. However, the NEXAFS signal from the Cu single crystal was recorded in the bulk-sensitive, total fluorescence yield (TFY) detection mode with a Hamamatsu GaAsP photodiode (G2119) to obviate uncertainties about surface cleanliness. All spectra were normalized to the incident photon flux measured simultaneously. The photon-energy resolution at the Cu L- and O K-edges was better than 1.0 and 0.3 eV, respectively. The photon energy was calibrated to the thresholds of the Cu L_3-edge absorption at 931.3 eV and O K-pre-edge transition at 530.2 eV using a CuO reference sample.[26] After energy calibration, spectra were normalized to the magnitudes of the absorption-edge jumps.[19] The NEXAFS measurements were performed at room temperature.

Results and Discussion

The experimental conditions adopted for growing OQDs on various $SrTiO_3$(001) surfaces and the effective OQD thickness are given in Table 1. In all cases, the total copper content in the OQDs measured by QCOs agrees with that determined by RBS along with SIMNRA simulations.[24] However, the effective OQD thickness depends on the oxygen content in the film in addition to the copper content. Because the major phase of the copper oxide is Cu_2O, the nominal effective OQD thicknesses given in Table 1 were determined using the bulk density of Cu_2O coupled with the total Cu content in the OQDs measured by QCOs and RBS along with SIMNRA simulations. Although the samples are identified by their effective thicknesses throughout, the vertical height of an individual cluster from a particular sample is typically larger than the effective thickness of the film.

AFM images of 2.4-nm-thick OQD grown on clean $SrTiO_3$(001) surfaces at 875 K with $p(O_2)$ of 1.2×10^{-6} Torr and at 800 K with $p(O_2)$ of 7.1×10^{-7} Torr are shown in parts (a) and (c), respectively, of Figure 1. The average lateral size and vertical height of the OQDs discussed below were obtained from the AFM data. The OQDs grown at 875 K show continuous film structure with wide terraces. The OQDs grown at 800 K with lower $p(O_2)$, however, show many three-dimensional nanodots with an average lateral size of ~15−20 nm. The average vertical height of the clusters from the surface of the $SrTiO_3$(001) substrate is 3.7 nm. The three-dimensional nanostructures appear to be well-isolated on the surface, and their lateral size decreased to about 5−10 nm for 0.6-nm-thick OQDs (Figure 1b). In addition, the average vertical height is also reduced to 2.1 nm. In contrast, when the film thickness was increased to 3.6 nm under the same growth conditions, the average lateral size and vertical height increased to 25−30 and 8.5 nm, respectively (Figure 1d). To demonstrate the effect of surface preparation on the physical dimensions of the OQDs, the AFM images of OQDs grown on chemically etched TiO_x-terminated and Au^{2+} ion-implanted surfaces under the same experimental growth conditions are shown in parts (e) and (f), respectively, of Figure 1. The average lateral size of the OQDs generated on the chemically etched TiO_x surface is 45 nm and these nanostructures show somewhat defined edges as previously reported.[18] The average vertical height also increased to about 10.0 nm. However, the OQDs grown on the ion-implanted $SrTiO_3$-(001) surface show a rough surface due to heavy Au^{2+} ion irradiation with much smaller OQD size. The average lateral size of these quantum dots is in the range of ~8−10 nm.

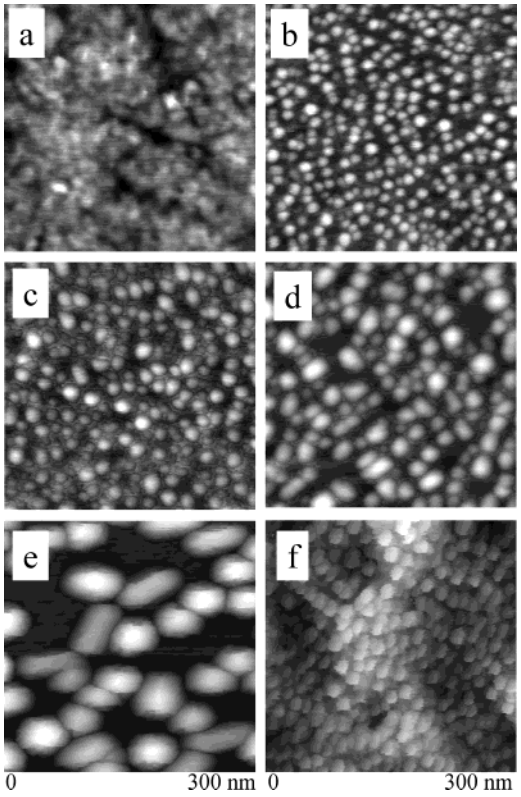

Figure 1. Atomic force microscope (AFM) image of (a) 2.4-nm OQDs grown on a clean $SrTiO_3$(001) surface at 875 K with $p(O_2)$ of 1.2×10^{-6} Torr. Images (b), (c), and (d) are for 0.6-, 2.4-, and 3.6-nm-thick OQDs grown at 800 K with $p(O_2)$ of ~7.0×10^{-7} Torr on clean $SrTiO_3$(001) surfaces, respectively. Images (e) and (f) are for 2.4-nm-thick OQDs grown at 800 K with $p(O_2)$ of ~7.0×10^{-7} Torr on TiO_x-terminated and Au^{2+} ion-implanted $SrTiO_3$(001) surfaces, respectively.

The Cu $L_{2,3}$- and O K-edge NEXAFS spectra for OQDs grown on clean $SrTiO_3$(001) surfaces at 875 K, $p(O_2) = 1.2 \times 10^{-6}$ Torr, and 800 K, $p(O_2) = 7.1 \times 10^{-7}$ Torr,

(26) Tjeng, L. H.; Chen, C. T.; Cheong, S. W. *Phys. Rev. B* **1992**, *45*, 8205.

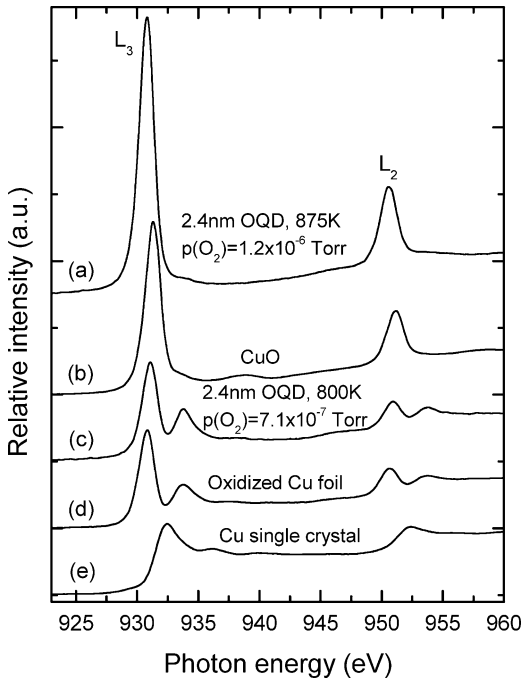

Figure 2. Cu $L_{2,3}$-edge NEXAFS for 2.4-nm-thick OQDs grown on a clean $SrTiO_3(001)$ surface (a) at 875 K with $p(O_2)$ of 1.2×10^{-6} Torr and (c) at 800 K with $p(O_2)$ of 7.1×10^{-7} Torr. The curves (b), (d), and (e) are for the reference materials CuO, an oxidized Cu foil (Cu_2O), and a Cu single crystal (collected in TFY), respectively.

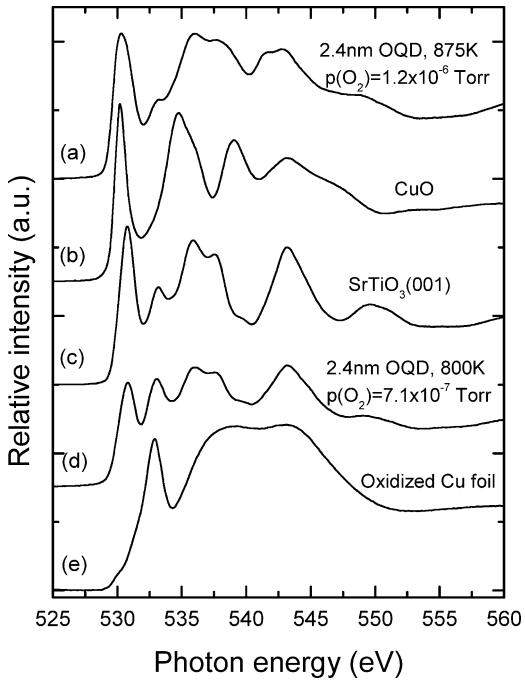

Figure 3. O K-edge NEXAFS for 2.4-nm-thick OQDs grown on a clean $SrTiO_3(001)$ surface (a) at 875 K with $p(O_2)$ of 1.2×10^{-6} Torr and (d) at 800 K with $p(O_2)$ of 7.1×10^{-7} Torr. The curves (b), (c), and (e) are for the reference materials CuO, $SrTiO_3(001)$, and an oxidized Cu foil (Cu_2O), respectively.

are compared with spectra from reference materials [a Cu single crystal, CuO, and an oxidized Cu foil (primarily Cu_2O)] in Figures 2 and 3, respectively. The oxygen K-edge NEXAFS from a clean $SrTiO_3(001)$ substrate is also included in Figure 3 for comparison. The Cu $L_{2,3}$- and O K-edge NEXAFS for 2.4-nm-thick OQDs grown on a clean $SrTiO_3(001)$ surface at 875 K with oxygen $p(O_2)$ of 1.2×10^{-6} Torr, and at 825 K, with $p(O_2)$ of 9.2×10^{-7} Torr, show exactly the same features. Thus, NEXAFS spectra are shown only for the former. The near-edge spectral feature characteristic of Cu_2O in the O K-edge spectra for the oxidized Cu foil agrees with the previously reported spectra for Cu_2O,[27,32,33] except for the presence of a weak shoulder that can be identified as originating from CuO. Although the oxidized Cu foil contains CuO only as an impurity, the Cu L-edge NEXAFS spectra show transitions characteristic of both Cu(II) and Cu(I), resulting from the large absorption cross section for Cu(II) compared to that of Cu(I).[27,29,34] The large cross-sectional differences observed at the Cu L-edge are evident in the O K-edge spectra in which the oxygen-related feature of CuO has a similar cross section to that of Cu_2O. The energy shifts observed at the Cu L_3-edge (~2.5 eV) and O K-edge (~2.7 eV) NEXAFS spectra between Cu_2O from the oxidized Cu foil and CuO are in good agreement with those reported previously.[26,27] This suggests that the surface of the oxidized Cu foil contains mainly Cu_2O with a minor impurity of CuO.[26−33] The intense and broad spectral profile in the postedge region (535−550 eV) originates from the CuO impurity and the overall amorphous nature of the oxidized film on the Cu foil. Thus, with recognition of the features specific to the CuO impurities and utilization of previous spectral assignments,[26−33] the oxidized Cu foil serves as an acceptable Cu_2O [Cu(I)] reference for the current investigation.

On the basis of earlier reports concerning CuO and Cu_2O, the following assignments are made for transitions in the Cu $L_{2,3}$- and O K-edge NEXAFS spectra.[26−31] The ground state of CuO consists mainly of p^6d^9 with a small contribution from p^5d^{10}. Thus, the bands centered at 951.2 and 931.3 eV labeled L_2 and L_3 for CuO can be assigned to $(2p_{1/2,3/2})^{-1}p^6d^{10}$, where $(2p_{1/2,3/2})^{-1}$ denotes a hole in the Cu $2p_{1/2}$ or $2p_{3/2}$ state (Figure 2). A weak shoulder on the high-energy side of the L_3 peak at ~933.8 eV originates from a Cu_2O impurity. The sharp band occurring at ~530.2 eV in O K-edge NEXAFS for CuO is assigned to $(1s)^{-1}p^6d^{10}$, where $(1s)^{-1}$ denotes a hole in the O 1s shell (Figure 3).

In Cu_2O, copper is Cu(I), with a completely filled 3d shell. The ground state of Cu_2O is a combination of p^6d^{10}, $p^6d^9sp^1$, and $p^5d^{10}sp^1$, in which the second configuration contributes strongly to Cu $L_{2,3}$ spectra. Thus, the bands centered at 953.7 and 933.8 eV labeled as L_2 and L_3, respectively, for the oxidized Cu foil (Cu_2O) can be assigned to $(2p_{1/2,3/2})^{-1}p^6d^{10}sp^1$ (Figure 2). The energy shift of ~2.5 eV observed at the Cu L_3-edge of Cu_2O

(27) Grioni, M.; van Acker, J. F.; Czyžyk, M. T.; Fuggle, J. C. *Phys. Rev. B* **1992**, *45*, 3309.
(28) Nachimuthu, P.; Chen, J. M.; Liu, R. S.; Waje, T. B.; Gopalakrishnan, I. K.; Yakhmi, J. V. *J. Chem. Soc.-Dalton Trans.* **1999**, 2065.
(29) Finazzi, M.; Ghiringhelli, G.; Tjernberg, O.; Ohresser, P.; Brookes, N. B. *Phys. Rev. B* **2000**, *61*, 4629.
(30) Karppinen, M.; Kotiranta, M.; Yamauchi, M.; Nachimuthu, P.; Liu, R. S.; Chen, J. M. *Phys. Rev. B* **2001**, *63*, U568.
(31) Karis, O.; Magnuson, M.; Wiell, T.; Weinelt, M.; Wassdahl, N.; Nilsson, A.; Mårtensson, N.; Holmström, E.; Niklasson, A. M. N.; Eriksson, O.; Johansson, B. *Phys. Rev. B* **2001**, *63*, 113401, and references therein.
(32) Knop-Gericke, A.; Hävecker, M.; Schedel-Niedrig, T.; Schlögl, R. *Catal. Lett.* **2000**, *66*, 215.
(33) Knop-Gericke, A.; Hävecker, M.; Schedel-Niedrig, T.; Schlögl, R. *Top. Catal.* **2000**, *10*, 187.
(34) Carniato, S.; Luo, Y.; Ågren, H. *Phys. Rev. B* **2001**, *63*, 85105.

compared to CuO suggests this additional energy is required to promote an electron to the 4sp states instead of to the 3d subshell, which is filled for Cu(I). This conclusion is supported by the O K-edge NEXAFS for CuO and Cu_2O ($\Delta E \sim 2.7$ eV).[26,27,29] The sharp peak at ~532.9 eV in the O K-edge NEXAFS for the oxidized Cu foil (Cu_2O) in Figure 3 is assigned to $(1s)^{-1}p^6d^{10}sp^1$. Bands centered at ~950.6 and 930.8 eV in the oxidized Cu foil NEXAFS are attributed to the $L_{2,3}$-edges, respectively, of Cu(II) present as impurity.[31] Comparison of transition energies obtained in this investigation for Cu $L_{2,3}$- and O K-edges of CuO and Cu_2O with earlier reports shows general agreement within experimental error.[26−34] In addition, as the absorption cross section for excitation from 2p → 4s is expected to be weaker in Cu_2O compared to 2p → 3d to CuO, the Cu L-edge jumps were observed to be larger for the former and smaller for the latter, in agreement with earlier reports.[27,29,34]

Large enhancements in the intensities of the transitions at the Cu $L_{2,3}$-edges are apparent for OQDs grown at 875 K with $p(O_2)$ of 1.2×10^{-6} Torr, as in CuO, in contrast to OQDs grown at 800 K with $p(O_2)$ of 7.1×10^{-7} Torr (Figure 2). The transition energies for the $L_{2,3}$-edges of OQDs grown at 875 K with $p(O_2)$ of 1.2×10^{-6} Torr also shift ~0.5 eV toward lower energy compared to that of crystalline CuO, due to its nanostructural phase resulting in a weaker covalent bonding between the copper and oxygen atoms, unlike in crystalline CuO. This is supported by an earlier study of nanocrystalline CeO_2 by X-ray absorption spectroscopy at the Ce L_3-edge, where the energy shift toward lower energy for the transition to the $(2p_{3/2})^{-1}p^5f^1d^1$ final state is attributed to a decrease of covalence between cerium and oxygen atoms with decreasing particle size.[35] In the O K-edge NEXAFS for the OQDs on the $SrTiO_3$(001) substrates shown in Figure 3, the spectral responses from the substrates decrease due to the presence of OQD overlayers that partially mask the $SrTiO_3$(001) surfaces.[36]

Unlike the Cu $L_{2,3}$-edges, the O K-edge NEXAFS signal is composed of contributions from the OQDs and the oxygen from the $SrTiO_3$(001) substrate. To isolate the spectral contribution from the OQDs, O K-edge NEXAFS obtained for a clean $SrTiO_3$(001) surface (~50% in magnitude) is subtracted from the spectra obtained for 2.4-nm-thick OQDs on $SrTiO_3$(001) surfaces. The resulting difference spectra are reproduced in Figure 4 for OQDs grown on different $SrTiO_3$ surfaces and with various preparation conditions. The O K-edge NEXAFS difference spectra of OQDs grown at 875 K with $p(O_2)$ of 1.2×10^{-6} Torr has a spectral profile similar to that of CuO. However, the band occurring at 530.2 eV for CuO broadens and shifts ~0.2 eV to lower energy for OQD. The line broadening and the edge shift can be rationalized by considering the amorphous nature of the sample. Similar edge shifts are found for Cu $L_{2,3}$-edges as discussed earlier, although the shifts differ in magnitude. These results suggest OQDs grown on clean $SrTiO_3$(001) surfaces at 825 K and higher with $p(O_2)$ of 9.0×10^{-7} Torr or greater contain mostly CuO.

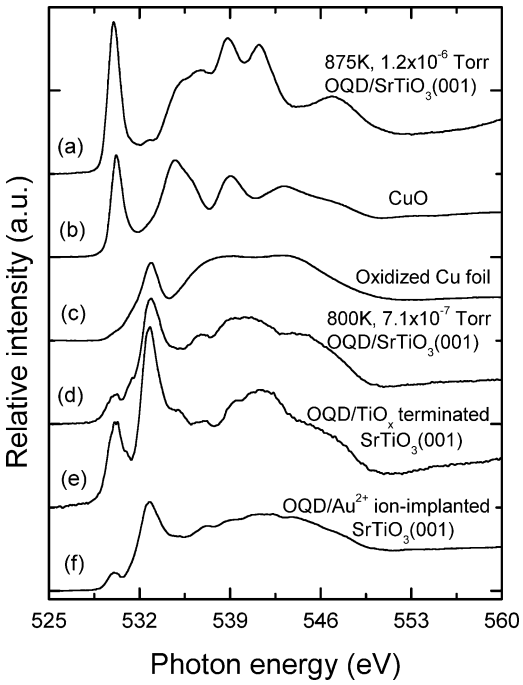

Figure 4. O K-edge NEXAFS difference spectra for 2.4-nm-thick OQDs grown on a clean $SrTiO_3$(001) surface (a) at 875 K with $p(O_2)$ of 1.2×10^{-6} Torr and (d) at 800 K with $p(O_2)$ of 7.1×10^{-7} Torr. The curves (e) and (f) for 2.4-nm-thick OQDs grown at 800 K with $p(O_2)$ of 7.1×10^{-7} Torr on TiO_x-terminated and Au^{2+} ion-implanted $SrTiO_3$(001) surfaces, respectively. The O K-edge spectra for reference materials (b) CuO and (c) an oxidized Cu foil (Cu_2O) are included for comparison.

In contrast, both Cu L- and O K-edge NEXAFS for the 2.4-nm-thick OQDs grown on a clean $SrTiO_3$(001) surface at 800 K with $p(O_2)$ of $\sim 7.0 \times 10^{-7}$ Torr show different features. The intensities of the Cu $L_{2,3}$-edges at 953.6 and 933.7 eV characteristic of Cu_2O are significantly enhanced as in the oxidized Cu foil (Cu_2O) (Figure 2). However, the $L_{2,3}$-edge features at 950.8 and 931.1 eV corresponding to CuO still exist, although weak. These results strongly suggest 2.4-nm-thick OQDs grown on a clean $SrTiO_3$(001) surface at 800 K with $p(O_2)$ of $\sim 7.0 \times 10^{-7}$ Torr contain largely Cu_2O. Furthermore, the O K-edge NEXAFS difference spectrum shows features very similar to those of the oxidized Cu foil (Cu_2O), although the presence of a very weak pre-edge feature at 530.2 eV corresponding to CuO suggests that the OQDs formed at 800 K and $p(O_2) = 7.0 \times 10^{-7}$ Torr contain CuO as an impurity (Figure 4).

To establish the effect of film thickness on the formation of OQDs, different thicknesses (0.6, 2.4, and 3.6 nm) of OQD were grown on clean $SrTiO_3$(001) surfaces at 800 K with $p(O_2)$ of $\sim 7.0 \times 10^{-7}$ Torr. The NEXAFS measured both at the Cu L- and O K-edges are shown in Figures 5 and 6, respectively. Intensities of the Cu $L_{2,3}$ transitions characteristic of Cu_2O increase significantly with thickness, in comparison to transitions corresponding to CuO. Similar effects are apparent in the O K-edge spectra.[36] As discussed earlier, the OQDs containing CuO and Cu_2O show characteristic pre-edge features at 530.0 and 532.9 eV, respectively, in the O K-edge NEXAFS. These transitions overlap with transitions occurring from the $SrTiO_3$ substrate depending on the concentrations of the constituents in the overlayer.[26−31,36] Thus, a decrease in intensity of the

(35) Nachimuthu, P.; Shih, W. C.; Liu, R. S.; Jang, L. Y.; Chen, J. M. *J. Solid State Chem.* **2000**, *149*, 408.
(36) Fuchs, D.; Adam, M.; Schweiss, P.; Gerhold, S.; Schuppler, S.; Schneider, R.; Obst, B. *J. Appl. Phys.* **2000**, *88*, 1844.

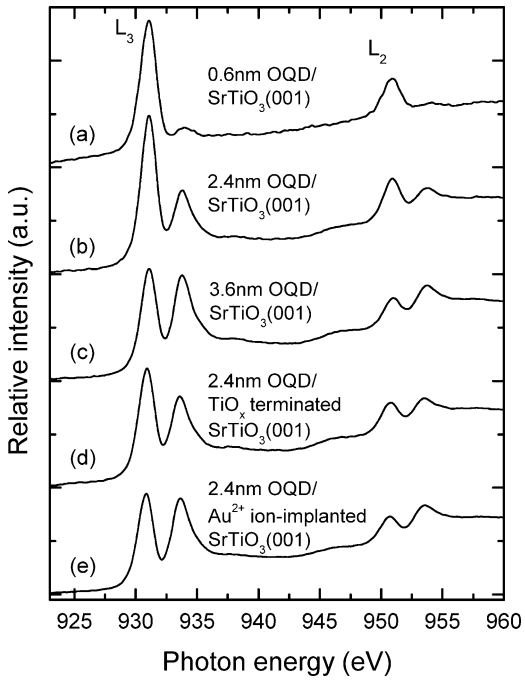

Figure 5. Cu $L_{2,3}$-edge NEXAFS for (a) 0.6-, (b) 2.4-, and (c) 3.6-nm-thick OQDs grown on a clean $SrTiO_3(001)$ surface at 800 K with $p(O_2)$ of $\sim 7.0 \times 10^{-7}$ Torr. Curves (d) and (e) are for 2.4-nm-thick OQDs grown on TiO_x-terminated and Au^{2+} ion-implanted $SrTiO_3(001)$ surfaces at 800 K with $p(O_2)$ of $\sim 7.1 \times 10^{-7}$ Torr, respectively.

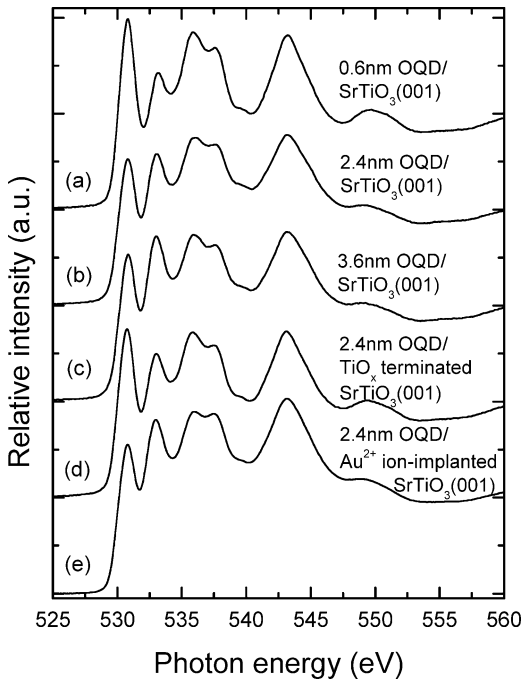

Figure 6. O K-edge NEXAFS for (a) 0.6-, (b) 2.4-, and (c) 3.6-nm-thick OQDs grown on a clean $SrTiO_3(001)$ surface at 800 K with $p(O_2)$ of $\sim 7.0 \times 10^{-7}$ Torr. Curves (d) and (e) are for 2.4-nm-thick OQDs grown on TiO_x-terminated and Au^{2+} ion-implanted $SrTiO_3(001)$ surfaces at 800 K with $p(O_2)$ of $\sim 7.1 \times 10^{-7}$ Torr, respectively.

transition at 530.8 eV with no corresponding change in transition energies and line shapes with increasing OQD thickness suggests the film thickness has increased, but there is no additional formation of CuO. In contrast, an increase in the intensity of the transition at 533.1 eV, with a slight shift to lower energy, indicates the formation of Cu_2O occurs exclusively with increasing OQD thickness. These results suggest there is a strong interaction between the $SrTiO_3(001)$ surface and the OQD overlayer, which induces oxidation of Cu(I) and hence the formation of Cu(II) for the first few monolayers. The interaction weakens with increasing thickness of the OQDs and results in the exclusive formation of copper(I) oxide at the top layers. This effect is known for self-assembled quantum dots and their electronic and structural properties are strongly influenced by the substrate on which the quantum dots are formed.[3−6,8,9] Clearly, the OQDs are influenced by the $SrTiO_3(001)$ substrate in the present case. However, identifying the exact nature of the interactions between OQD and the $SrTiO_3(001)$ substrate warrants further investigation.

To further elucidate the influence of the substrate on the formation of OQDs, 2.4-nm-thick OQDs were grown on TiO_x-terminated and Au^{2+} ion-implanted $SrTiO_3(001)$ surfaces at 800 K with $p(O_2)$ of $\sim 7.0 \times 10^{-7}$ Torr. These OQDs were compared to the clusters grown on clean $SrTiO_3(001)$ surfaces under the same experimental conditions. The corresponding NEXAFS spectra collected at the Cu L- and O K-edges are included in Figures 5 and 6, respectively. The intensities of transitions in the Cu L- and O K-edge NEXAFS characteristic of Cu_2O are significantly enhanced, compared to the intensities of the transitions from CuO, by modifying the surface of the $SrTiO_3(001)$ substrate. The intensities of the CuO signals are reduced most preferentially for Au^{2+} ion-implanted, and then TiO_x-terminated, followed by the usual behavior of the clean substrate (Figure 5). Thus, surface modification of the $SrTiO_3(001)$ substrate facilitates formation of Cu_2O. In addition, the transitions in the NEXAFS spectra show a slight shift ($\sim$0.2 eV) to lower energy for OQDs grown on TiO_x-terminated and ion-implanted surfaces, compared to a clean $SrTiO_3$-(001) surface, suggesting the interaction between the substrate and OQDs becomes weaker. These results provide strong evidence for the presence of a small fraction of Cu(II), irrespective of the surface of the substrate and/or the thickness of the OQDs, due to substrate interaction with the first few monolayers of the OQDs.

The Cu $2p_{3/2}$ core-level XPS spectra from 1.2-, 2.4-, and 3.6-nm-thick OQDs on clean $SrTiO_3$ substrates is presented in Figure 7. These spectra show peaks at 932.5 and $\sim$934.2 eV and shake-up features centered around $\sim$942.5 eV. The binding energies of Cu $2p_{3/2}$ core levels are 932.7 eV for metallic Cu,[37] 932.5 eV for Cu-(I),[38] and 933.5 eV for Cu(II).[39] Although it is difficult to resolve the peaks from metallic Cu and Cu(I) in XPS spectra, the binding energy difference between Cu(I) and Cu(II) is quite large ($\Delta E \sim 1$ eV) and can be clearly resolved in an XPS spectrum containing a mixture of Cu(I) and Cu(II). In addition, the shake-up feature ($\sim$942.5 eV) associated with the Cu(II) is unique and this feature can be effectively used to identify and quantify Cu(II). The XPS results for the OQD obtained in this study show the binding energy for Cu(II) is shifted to significantly higher energies compared to the literature value of 933.5 eV (shift $\sim$0.7 eV) from strong

(37) Vasquez, R. P. *Surf. Sci. Spectra* **1993**, *2*, 55.
(38) Vasquez, R. P. *Surf. Sci. Spectra* **1998**, *5*, 257.
(39) Vasquez, R. P. *Surf. Sci. Spectra* **1998**, *5*, 262.

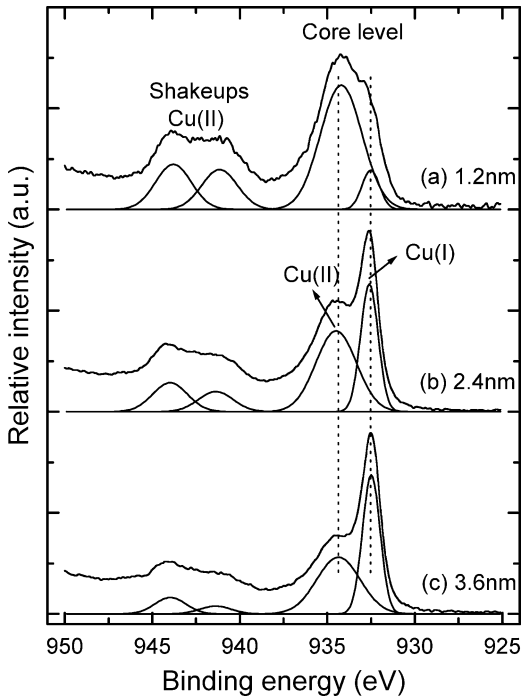

Figure 7. Cu $2p_{3/2}$ XPS spectra for (a) 1.2-, (b) 2.4-, and (c) 3.6-nm-thick OQDs grown on a clean $SrTiO_3(001)$ surface at 800 K with $p(O_2)$ of $\sim 7.0 \times 10^{-7}$ Torr. The X-ray source used was an Al Kα anode ($h\nu = 1486.6$ eV), and the photoelectrons were collected at a 90° takeoff angle (normal emission).

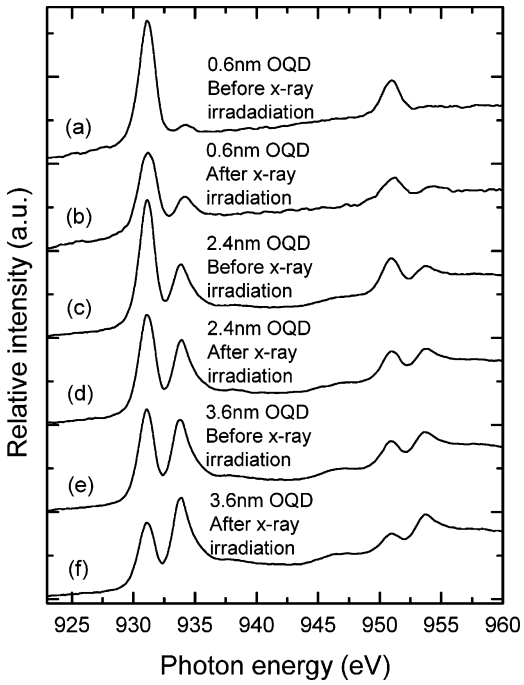

Figure 8. Cu $L_{2,3}$-edge NEXAFS for (a,b) 0.6-, (c,d) 2.4-, and (e,f) 3.6-nm-thick OQDs grown on a clean $SrTiO_3(001)$ surface at 800 K with $p(O_2)$ of $\sim 7.0 \times 10^{-7}$ Torr. The curves (a), (c), and (e) are prior to X-ray irradiation and curves (b), (d), and (f) are after 1 h of soft X-ray irradiation at 900 eV.

interactions between Cu(II) and the substrate. The Cu $2p_{1/2}$ XPS spectra from these films (not shown) show similar shifts in binding energy for Cu(II). Finally, the intensities related to the Cu(II) features decrease with increasing thickness and are consistent with the aforementioned NEXAFS results.

To ascertain the photochemical properties of the OQDs, each sample was irradiated with 900-eV soft X-ray radiation for about an hour. Before and after X-ray irradiation, NEXAFS spectra were measured both at the Cu L- and O K-edges. As a representative example, Cu L-edge NEXAFS before and after irradiation for the 0.6-, 2.4-, and 3.6-nm-thick OQD grown on clean $SrTiO_3(001)$ substrates at 800 K with $p(O_2)$ of $\sim 7.0 \times 10^{-7}$ Torr are given in Figure 8. The intensities of transitions in the Cu L-edge NEXAFS characteristic of Cu_2O are significantly enhanced in comparison to those of transitions from CuO after irradiation, irrespective of the thickness of the OQDs. These intensity variations in the Cu L-edge NEXAFS clearly indicate Cu(II) is reduced to Cu(I) under X-ray irradiation. Similar observations were made at the Cu L-edge for different particle sizes of CuO/Cu_2O on the surface of SiO_2/Si(001) substrates by XPS.[40,41] This was attributed to X-ray-induced reduction of Cu(II) initially formed at the surface by spin-coating Cu(II) acetate solutions with varying concentrations. The degree of Cu(II) reduction correlates with particle size because smaller particles are more susceptible to reduction consistent with their larger surface area, leading to increased effects from irradiation. Unlike the Cu L-edge, O K-edge NEXAFS for OQDs in the present study does not exhibit significant changes following irradiation, suggesting the substrate mediates effects of irradiation via reactions between substrate and Cu atoms in the OQDs.

Conclusions

The 2.4-nm-thick OQD grown on clean $SrTiO_3(001)$ surfaces at 825 K and higher with $p(O_2)$ of 9.0×10^{-7} Torr or greater contain mostly CuO. In contrast to this result, the 2.4-nm-thick OQDs grown on a clean $SrTiO_3$-(001) surface at a temperature of 800 K with $p(O_2)$ of $\sim 7.0 \times 10^{-7}$ Torr largely contains Cu_2O, although CuO is present as a minor impurity. A strong interaction between the $SrTiO_3(001)$ surface and the first few monolayers of the OQDs, which induces the formation of Cu(II), is observed. However, the interaction weakens with increasing thickness of OQDs, resulting in the exclusive formation of Cu(I) in the top layers. Modifying the substrate surface using chemical treatment and/or energetic Au^{2+} ion-beam irradiation can mitigate the influence of substrate on OQD formation. Examination of the photochemical properties of these OQDs by prolonged soft X-ray irradiation under vacuum indicates the Cu(II), present as a minor impurity, is reduced to Cu(I).

Acknowledgment. This work was supported by the Nevada NSF EPSCoR RING-TRUE program under Award No. EPS-9977809 and the DOE EPSCoR State-National Laboratory Partnership program under Award No. DE-FG02-01ER45898. Parts of the work were conducted in the Environmental Molecular Sciences Laboratory, a U.S. Department of Engergy (DOE) user facility operated for the DOE by Pacific Northwest National Laboratory under Contract No. DE-AC06-76RLO-1830. Dr. Y. J. Kim's travel was supported in

(40) Brookshier, M. A.; Chusuei, C. C.; Goodman, D. W. *Langmuir* **1999**, *15*, 2043.
(41) Kirsch, P. D.; Ekerdt, J. G. *J. Appl. Phys.* **2001**, *90*, 4256.

part by the Korea Science and Engineering Foundation through the Advanced Materials Research Center for a Better Environment at Hanbat National University, Korea. The Advanced Light Source is operated by the Director, Office of Science, Office of Basic Energy Sciences, Division of Materials Science of the U.S. DOE under Contract No. DE-AC03-76SF00098 at LBNL. Part of this work (D.K.S.) was supported by the Director, Office of Science, Office of Basic Energy Sciences, Chemical Sciences, Geosciences and Biosciences Division of the U.S. DOE under Contract No. DE-AC03-76SF00098 at LBNL. The authors gratefully acknowledge helpful suggestions from Y. Liang from Motorola.

CM021757N